Gas Dynamic Considerations for Performance of Nanocluster Deposition System

Petr A. Skovorodko[a], Simon A. Brown[b] and Domagoj Belić[b]

[a]*Institute of Thermophysics, 630090, Novosibirsk, Russia*
[b]*MacDiarmid Institute of Advanced Materials and Nanotechnology*
Department of Physics and Astronomy, University of Canterbury, Christchurch, New Zealand

Abstract. Numerical simulations of the gas flow and cluster velocities in a UHV compatible nanocluster deposition system were performed in order to understand the problems of optimization of the cluster deposition rate. Skimmer geometry was initially identified as the key factor in defining the cluster velocity: our modeling suggested that using skimmers of a greater internal angle should lead to higher cluster velocities. However, the experimental results revealed only a minor enhancement in the cluster velocity. The lack of an effect of the change in skimmer geometry was attributed to the decelerating effect of the background gas in the mass selection chamber. When this effect was taken into consideration, the simulation results described the observed cluster behavior to a much better degree. The experiments and simulations both show a general trend for the cluster velocity to decrease as the cluster size is increased, for all the skimmer geometries used.

Keywords: cluster velocity, UHV sputtering, mass selection, skimmer, Navier-Stokes equations, DSMC, AgAu.
PACS: 07.77.-n, 29.25.-t, 36.40.Wa, 37.20.+j, 41.85.Qg, 47.40.Ki, 47.45.-n, 47.60.Kz, 63.22.Kn

INTRODUCTION

Nanoclusters have been studied for many years because they allow exploration of a wide range of new physical and chemical phenomena. Clusters can be prepared in several different ways but the inert gas aggregation technique [1] is especially attractive because it allows cluster formation in a clean environment free of contamination and is amenable to cluster deposition in order to fabricate nano-electronic devices [2]. One of the outstanding issues, however, is that in order to allow efficient device fabrication it is critical that the maximum flux of clusters is achieved. Until now the complexity of the cluster deposition system (which incorporates several nozzles and skimmers), and the difficult pressure regimes (typical pressures between first nozzle and skimmer are in the range ~ 0.1-1mbar), mean that it has not been possible to optimize the cluster throughput via modeling. Here we report the first attempts to model the gas and cluster flow through the system.
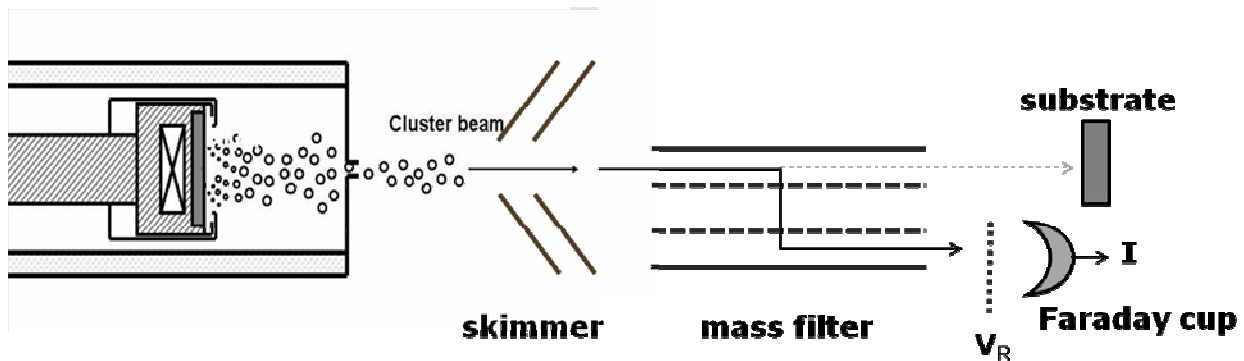

FIGURE 1. Schematic diagram of a 4-stage UHV magnetron sputtering system used for production of alloy clusters and velocity measurements. Distance between the skimmer and the Faraday cup is approximately 1m.

EXPERIMENTAL

A 4-stage ultra-high vacuum (UHV) compatible magnetron sputtering cluster deposition system (Fig. 1) is used for fabrication of clusters by means of inert gas aggregation (IGA) in a liquid-nitrogen-cooled source chamber (stage 1) [1]. In this work, sputtering is performed on an alloy target ($Ag_{0.85}Au_{0.15}$) which is water cooled to prevent melting. The experimental parameters used in these experiments were: sputter power: 25 W; aggregation length (target - nozzle distance): 8 cm; Argon flow rate: 50 - 350 sccm; temperature of the source chamber walls: ~77K. These parameters define the cluster size distribution leaving the source.

A continuous flow of Ar is maintained as the mixture of gas and clusters expands from the source into the mass-selection chamber (stage 3) through a pair of apertures (which define the cluster beam). In the differential pumping chamber (stage 2) located between the apertures (Fig. 2(a)) much of the inert gas is removed from the system. This process is intended to take place without disturbing the cluster beam, but of course the nozzle / skimmer geometry significantly impacts the gas/cluster flow - this influence is the main subject of this work. While, experimentally, it has been demonstrated [3] that the system provides an intense flux of clusters to a substrate (stage 4), until now calculations that allow us to understand the process in detail have not been available, and it has not been possible to know whether further optimization is possible.

The first aperture is a nozzle (Fig. 2(b)) which remained in place during the whole set of experiments. The design of this nozzle is the result of experimental trial and error over a period of about 10 years – this design seems to reliably give a high flux of particles with diameters in the range 5-10nm. The second aperture is a skimmer (Fig. 2(b)) whose design was changed in this work in order to optimize the cluster flux. The mass selection chamber is equipped with a mass filter that enables mass/size selection of the *charged* clusters [4, 5]. Before being collected by a Faraday cup, the mass-selected clusters have to pass through a steel mesh connected to external voltage supply that provides a retarding voltage V_R of the same sign as the charged clusters. This creates an energetic barrier for clusters: only those with kinetic energy equal or greater than the barrier will pass through the mesh and contribute to the signal I from the Faraday cup. Alternatively, one can switch the mass filter off which will result in the cluster beam passing straight to the deposition chamber (stage 4) where clusters can be deposited onto substrates for further characterization.
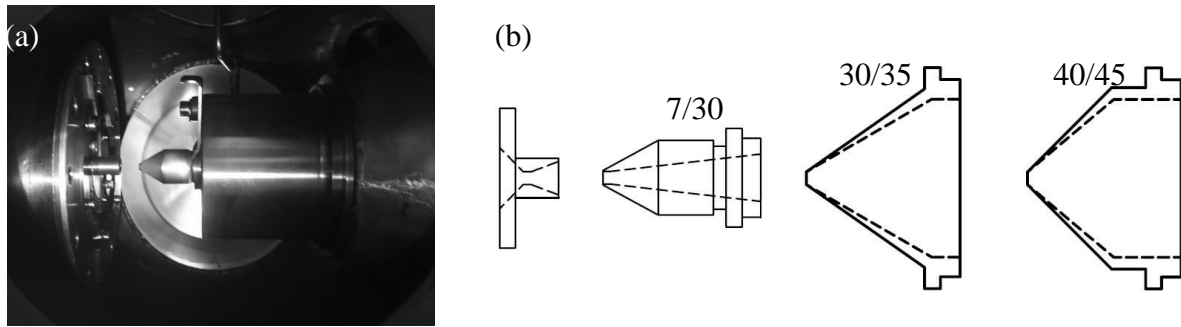

FIGURE 2. (a) Sideview photo of the pumping chamber showing the nozzle and 7/30 (internal/external angle) skimmer. The nozzle and skimmer are separated by 9 mm and are well aligned. (b) Schematic diagrams of the nozzle and skimmers used in our experiments.

Cluster Velocity Determination

Only charged clusters of sufficient kinetic energy E_K can pass the barrier imposed by the retarding voltage V_R and contribute to the measured current I:

$$\frac{1}{2}mv^2 = eV_R \tag{1}$$

The relation between the cluster velocity and retarding voltage is then:

$$v = 2\sqrt{\frac{3eV_R}{\pi\rho D^3}} \qquad (2)$$

The density of each cluster ρ is defined by the atomic composition ($Ag_{0.85}Au_{0.15}$) and the cluster diameter D is defined by the mass filter. A LabVIEW controlled Keithley voltage source/picoammeter was used for setting the retarding voltage V_R and measurement of the current I from the Faraday cup at the same time. I-V_R characteristics (an example is shown in Fig. 3) were obtained for various values of argon flow rate, cluster diameter, and nozzle-skimmer distance. The mean velocity of the clusters is determined by the "cut-off" retarding voltage $V_R{}^*$ which corresponds to the point where the following relation holds:

$$\frac{d^2I}{dV_R^2}\bigg|_{V_R=V_R{}^*} = 0 \qquad (3)$$

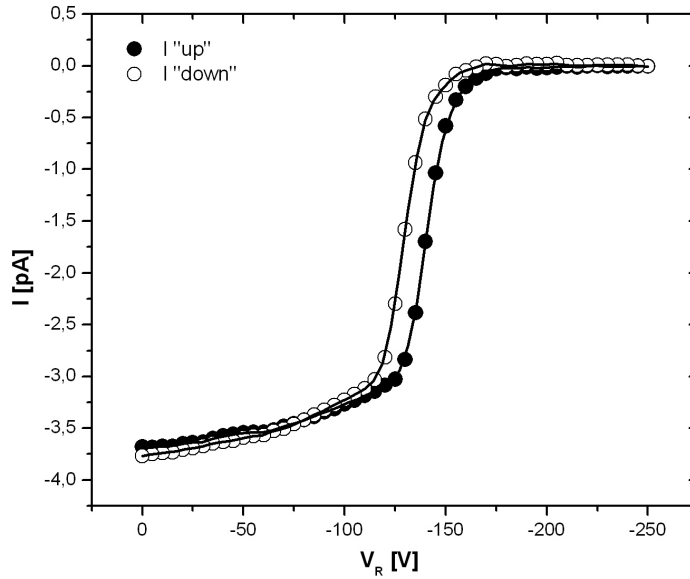**FIGURE 3.** Faraday cup signal I as a function of retarding voltage V_R for 7 nm clusters of $Ag_{0.85}Au_{0.15}$ and argon flow rate of 250 sccm. Negatively charged clusters were passed through the mass filter and the maximum current is obtained for zero retarding voltage. As the absolute value of the retarding voltage is increased ("up" branch), the energy barrier is raised resulting in the current dropping to zero. The retarding voltage is then decreased back to the initial value and the "down" branch is recorded. Values of the "cut-off" retarding voltage $V_R{}^*$ are defined by the steepest points on the slopes.

NUMERICAL SIMULATION

The numerical simulation of the cluster's motion in the carrier gas (argon) flow was divided into two separate stages.

The first one consists of the calculation of the dynamics of the carrier gas (argon) flow in the system. The flow in the nozzle used in the experiments was simulated in the frame of the full set of unsteady Navier-Stokes equations [6], with the subsonic part of the nozzle being included in the domain of simulation. The parameters of the nozzle are as follows: the diameter of throat section – 3.25 mm, the length of subsonic part – 6 mm, the length of supersonic part – 7 mm, the length of cylindrical part in the throat section – 2 mm, the inlet diameter – 15.5 mm, the exit diameter – 8.5 mm. The most difficult problem in simulating the flow of argon through the nozzle arises from poor knowledge of stagnation temperature T_0 as well as the nozzle wall temperature T_w in the experimental conditions when the stagnation pressure p_0 was measured. This problem is illustrated in Fig. 4 where the measured dependence of argon flow rate G on p_0 (curve 1) is compared with two theoretical curves obtained for $T_0 = T_w = 77$ K (curve 2) and $T_0 = T_w = 120$ K (curve 3). As it is seen from this figure, the assumption that $T_0 = T_w = 77$ K (i. e. the temperature of liquid nitrogen) contradicts the results of our measurements indicating that the real values of these

temperatures should be higher. We adopted the value $T_0 = T_w = 120$ K which provides a satisfactory match to the experimental curve, although the slope of theoretical (3) and experimental (1) curves is not the same (see Fig. 4).
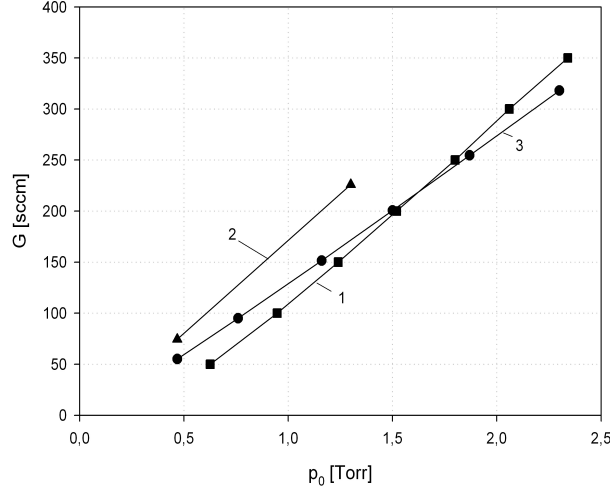

FIGURE 4. Measured (curve 1) and predicted (curves 2, 3) dependencies of $G(p_0)$ (see text).

The profiles of the parameters in the nozzle throat section were used as boundary conditions for simulations of further evolution of the flow inside and behind the nozzle and also in the region containing the skimmer. This simulation was made using the DSMC approach [7]. The nozzle wall was kept at temperature 120 K, while the skimmer wall was assumed to be at room temperature (290 K). The solid surfaces were assumed to be diffusely reflecting. The three skimmer geometries investigated are shown in Fig. 2b, the diameter of the inlet orifice of all the skimmers was 3.25 mm. The collisional properties of molecules were described by the VSS molecular model for a repulsive interaction potential between molecules ($\omega = 0.849656$, $\alpha_{VSS} = 1.77281$) [7].

In the second stage of the simulation the linear problem of the motion of clusters in the carrier gas flow was treated based on the expression for the free molecular drag coefficient of a spherical particle with diameter D moving with the velocity u in the equilibrium gas with density ρ_∞ and temperature T_∞ [7]:

$$C_D = \frac{4F}{1/2\rho_\infty u^2 \pi D^2} = \frac{2s^2+1}{\pi^{1/2}s^3}\exp(-s^2) + \frac{4s^4+4s^2-1}{2s^4}\mathrm{erf}(s) + \frac{2(1-\varepsilon)\pi^{1/2}}{3s}\left(\frac{T_w}{T_\infty}\right)^{1/2} \quad (4)$$

where F is the drag force, $s = u/\sqrt{2RT_\infty}$ is the speed ratio, ε is the fraction of specular reflection of molecules on the particle surface whose temperature is T_w. In the simulation we assume that $\varepsilon = 0$, $T_w = T_\infty$.

The simulations were performed for the $Ag_{0.85}Au_{0.15}$ clusters ($\rho = 11.82$ g/cm^3) used in the experiments. In this paper we will report only the results of the dependence of the cluster velocity on the gas flow rate and cluster size. The clusters are injected into the carrier gas flow field on the flow centerline near the inlet section of the nozzle with zero velocity.

RESULTS AND DISCUSSION

The carrier gas flow field inside and over the 7/30 skimmer (see Fig. 2b) was found to be strongly disturbed by internal and external skimmer interactions [8] resulting in the decrease of the gas velocity on the flow centerline behind the skimmer inlet. Hence two alternative skimmers 30/35 and 40/45 (see Fig. 2b) were developed and tested. The calculations reveal the clear advantage of these two skimmers over the 7/30 skimmer from the point of view of maximization of the cluster velocity. However, this maximization of the cluster velocity is not reproduced in the experiments.

Figure 5 illustrates the correlation between the cluster velocity and the cluster size for various skimmer geometries, keeping the argon flow rate fixed at 100 sccm. In the nominal geometry of the experiment the distance between the nozzle exit and skimmer inlet sections is $L = 9$ mm, but for the 45/40 skimmer the effect of setting $L = 6$ mm was also tested. The results of experimental measurements are shown by symbols while the numerical results

are shown by lines. For each of the considered regimes two calculated curves are plotted – without accounting for the decelerating effect of the background gas in the mass selection chamber (upper curves) and with taking this effect into account (lower curves). The values of background pressure p_b needed for latter calculations were either taken from experiments (for $p_b < 0.78$ mTorr) or from estimations based on the flow rate through the skimmer and the pumping speed of the used pump. The obtained velocity corresponds to the point on the flow centerline placed 1 m behind the right boundary of the domain of simulation which in turn was 75 mm downstream the nozzle exit section. Both experimental and numerical results show a tendency for the velocity to decrease for larger clusters, for all the skimmers used in our experiments. However, there is no obvious difference in the measured cluster velocities for the various skimmer geometries, which at first seems quite surprising. Our initial simulations suggested a significant increase of the cluster velocity for skimmers with greater internal angles (see upper calculated curves). The explanation for the unexpected experimental results lays in the fact that those skimmers also allow more inert gas to enter the mass selection chamber (stage 3), resulting in a higher background gas pressure. Consequently, clusters suffer more collisions with the argon gas in their path (a distance of 1 m) between the skimmer and the Faraday cup, decreasing their velocity to values close to those obtained for the original 7/30 skimmer. The lower calculated curves in Fig. 5 are in satisfactory agreement with the results of the experiments.
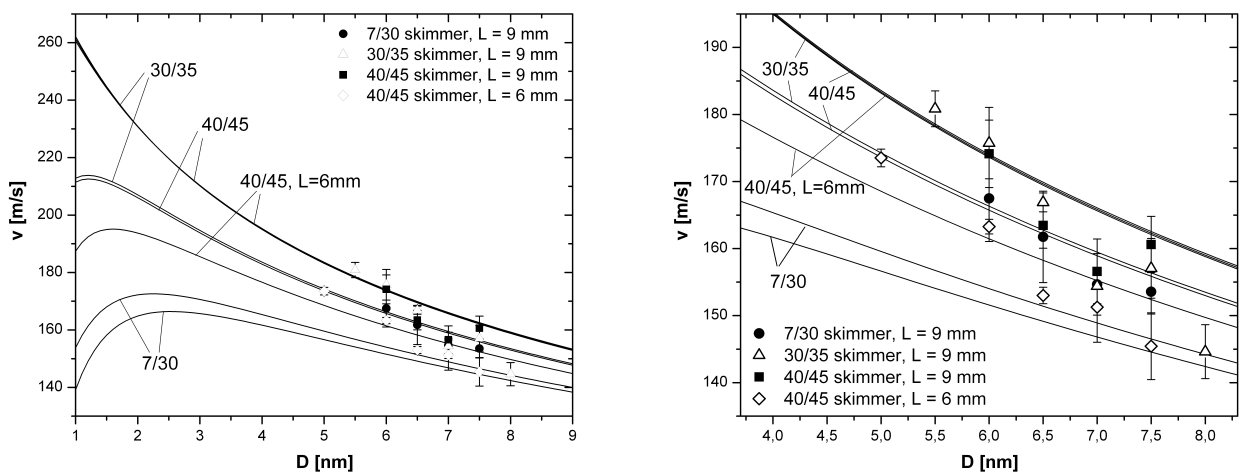

FIGURE 5. Dependence of the AgAu cluster velocity on the cluster size, for various skimmer geometries. Inert gas flow rate was set at 100sccm. A general trend of cluster velocity decrease with increasing cluster size is visible.
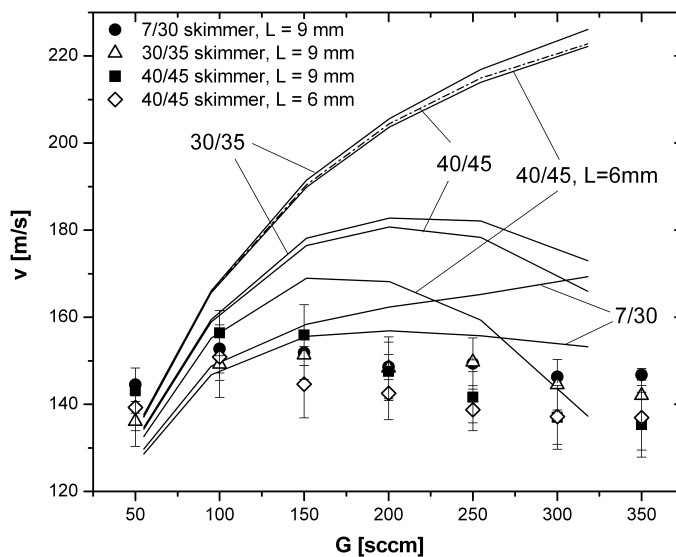

FIGURE 6. Dependence of the AgAu cluster velocity on the argon flow rate for various skimmer geometries.

In the case of 40/45 skimmer, when the nozzle-skimmer distance was reduced from 9mm to 6mm, a significant rise of mass selection chamber pressure was observed, which further decreased the cluster velocities, even below the values for the 7/30 skimmer, again suggesting the negative effect of the background pressure on the cluster velocity. With $L = 9$ mm the calculated flow rate through the 30/35 and 40/45 skimmers is about 3 times the flow rate through the 7/30 skimmer. Changing the distance L from 9 mm to 6 mm leads to a further 1.5 times increase of the flow rate through the skimmer. The differences between the upper and lower curves in Fig. 5 correlate well with these data.

One experimental solution for overcoming this problem is to install a turbo pump in the mass filter chamber with greater pumping speed than the current one (a Pfeiffer turbo pump TMU521 with a pumping speed of 520 l/s for nitrogen). Another is to reduce the size of the skimmer aperture.

The correlation between the cluster velocity and the inert gas flow rate was also investigated as illustrated in Fig. 6, where the corresponding experimental and numerical data for clusters with D = 7 nm are presented for the same regimes and in the same notations as in Fig. 5. The effect of the deceleration of the clusters by the background gas is very clear, especially at higher values of argon flow rate. Again the lower curves are in better agreement with the experiment compared to higher ones which, in turn, demonstrate the possible improvement in the velocity of the clusters that could be obtained using a pump with greater pumping speed.

CONCLUSION

The behavior of clusters carried by the inert gas flow inside a UHV cluster deposition system was studied using numerical simulations and compared with experimental results. The initial modeling suggested that using skimmers of greater internal angle could significantly increase the gas flow through the skimmer, leading to higher cluster velocities and ultimately to higher cluster fluxes. In order to investigate this, the velocity of size selected AgAu clusters was measured for various values of the argon flow rate and cluster size, for different skimmer geometries as well as for different nozzle-skimmer distances.

However, the experimental results did not show any significant increase in the cluster velocity when the new skimmers (with larger internal angles) were utilized. At first these results seemed very surprising However, this unexpected performance can be explained by the effect of the higher background gas pressure on the cluster velocity: due to collisions with argon gas molecules along their 1m long path inside the mass selection chamber, clusters tend to decelerate. Therefore, in the end any gain in the cluster velocity by using the skimmers with the larger internal angle is cancelled out by the higher background gas pressure in the mass selection chamber. Simple solutions that may solve this problem are to install a pump with the greater pumping speed or to decrease the size of the skimmer aperture.

ACKNOWLEDGMENTS

REFERENCES

1. R. Reichel, J. G. Partridge, A. D. F. Dunbar, S. A. Brown, O. Caughley, and A. Ayesh, *Journal of Nanoparticle Research*, **8**, 405 (2006).
2. J. Schmelzer jr, S. A. Brown, A. Wurl, M. Hyslop, and R. J. Blaikie, *Phys. Rev. Lett.*, **88**, 226802 (2002).
3. R. Reichel et al., *Appl. Phys. Lett.*, **89**, 213105 (2006).
4. B. v. Issendorf, R. E. Palmer, *Rev. Sci. Intrum.* **70**, 4497 (1999).
5. A. I. Ayesh et al., *Rev. Sci. Intrum.* **78**, 053906 (2007).
6. A. Broc, S. De Benedictis, G. Dilecce, M. Vigliotti, R. G. Sharafutdinov, and P. A. Skovorodko, *J. Fluid Mech.*, **500**, 211-237 (2004)
7. G.A. Bird, *Molecular Gas Dynamics and the Direct Simulation of Gas Flows*, Oxford, Clarendon Press, 1994.
8. J. B. Anderson, R. P. Andres and J. B. Fenn, "High Intensity and High Energy Molecular Beams," in *Advances in Atomic and Molecular Physics,* Vol. 1, edited by D. R. Bates and I. Estermann, New York: Academic Press, Inc., 1965, pp. 345-389.